

Verifying closed-loop performance before inserting a new controller

Arvin Dehghani, Brian D. O. Anderson and Sung H. Cha

Abstract—Consider a closed-loop interconnection of an unknown linear plant and a known linear stabilizing controller, and assume that some knowledge of the closed-loop system is available. Suppose—on the basis of that knowledge—the existing, still stabilizing, controller no longer provides a satisfactory closed-loop performance, and hence the use of a new controller appears attractive. This scenario is common in Multiple Model Adaptive Control and Iterative Identification and Control algorithms. Our results will provide assurance for the closed-loop performance before the insertion of a new controller, and complement our earlier results for guaranteeing closed-loop stability in advance.

I. INTRODUCTION

Let $[P, C_0]$ denote a feedback control interconnection consisting of a plant P and a controller C_0 . Further assume that the transfer function $P(s)$ is unknown while $C_0(s)$ is known. Let C_1 be a new controller designed to replace C_0 . We develop tests to verify if C_1 in place of C_0 will result in better closed-loop performance. The results are based on the knowledge of $C_0(s)$ and $C_1(s)$ and on data obtained from experiments on the closed-loop $[P, C_0]$, but not directly on P , and should exhibit significant tolerance of noise.

Many multi-controller adaptive switching algorithms do not explicitly rule out the possibility of placing a destabilising controller in the closed-loop [1], [2], [3]. Even if the new controller is ensured to be stabilising, it is not straightforward to verify whether the new controller will satisfy all the performance requirements and guarantee a better performing closed-loop. In adaptive control, it is very frequently the case that a model is explicitly or implicitly constructed, and the performance of the model is compared with the actual system. When the actual system comprises a plant in combination with a controller, the model may for example comprise an estimate of the plant obtained by identification in combination with the same controller. Or the model may be a desired closed-loop transfer function, and the actual system comprises the closed loop formed by the actual plant and the controller. Thus a measure of quality for the model is usually an *a priori* agreement. Note that a model may be a good model with one set of experimental conditions, but not with another set. This is important and becomes evident when one such scenario is discussed next.

Consider two transfer functions $P_1(j\omega)$ and $P_2(j\omega)$ and suppose that $|P_1(j\omega) - P_2(j\omega)| < 0.01 \forall \omega$. Then $P_2(j\omega)$

is reasonably deemed to be a good model of $P_1(j\omega)$. Let $P_1(s) = 1/(s + 1)$ and $P_2(s) = 1/(s + 1)(1s + 1)$, and compare their open-loop responses and their closed-loop responses when connected to two constant gain controllers $C_1 = -1$ and $C_2 = -100$. With C_1 the closed-loop responses are very similar, and with C_2 they are very different. Evidently, $P_2(s)$ is a good approximation of $P_1(s)$ in open loop, and remains so with a small feedback gain, but it is a poor approximation with a large feedback gain. Changing from having no controller in the loop to having a controller in the loop is another way of changing the experimental conditions, and there is then no guarantee that what was a good model will remain so. Similarly, if two closed-loop transfer functions are close, it does *not* imply that the two open-loop transfer functions are close. Even more crucially for adaptive control, if the closed-loop transfer functions are close with one controller, and the controller is changed, the two new closed-loop transfer functions may no longer be close. Such pitfalls are discussed in detail in [3].

Despite the rich volumes of literature on adaptive control algorithms, one cannot find an indication—at least to the point of verifying user-specific performance requirements—of research attempts to evaluate the closed-loop performance before a new controller C_1 is inserted into the loop. In fact, it is certainly not straightforward to even verify whether the new controller will maintain the closed-loop stability before it is switched in. In a series of works [4], [5], [6], we have recently developed stability results to infer if the introduction of a prospective controller C_1 into the loop will stabilise the unknown plant. The extensions of these stability results to include nonlinear cases appear in [7], [8], [9].

We shall propose novel analysis and experimental tests for verifying the closed-loop performance with the introduction of a new linear controller C_1 using a limited amount of noisy input-output experimental data obtained from the stable closed-loop $[P, C_0]$. Our proposed results utilise the existing stability verification tests of [4], [5], [6] to ensure the internal stability of $[P, C_1]$ and offer mechanisms for evaluating aspects of the closed-loop performance before inserting C_1 .

The structure of the paper is as follows. Section II collects and reviews the required definitions and notations from the relevant literature. In Section III, we shall present an overview of the relationships among the closed-loop performance measures before stating the problem of interest and a presenting a framework for the proposed experimental setting. This will lead to the development of the proposed performance analysis results of Section IV and experimental tests of Section V. Section VII contains concluding remarks and future research directions.

The authors are all with the Research School of Information Sciences and Engineering, The Australian National University, ACT 0200, Australia.

Brian D. O. Anderson is also with National ICT Australia Ltd., Locked Bag 8001, Canberra, ACT 2601, Australia.

Corresponding Author: Arvin Dehghani.

This work was supported in part by the ARC Discovery-Projects Grant DP1095290 and DP0664427.

II. PRELIMINARIES

The notations are standard and borrowed from [10], [11], [12]. We shall denote by \mathcal{H}_∞ the space of functions bounded and analytic in the open right-half complex plane, and the same function spaces with prefix \mathcal{R} their real-rational proper subspaces. The plant is assumed to be a MIMO linear time-invariant system (although at times we will restrict attention to scalar systems). The transfer function of the plant belongs to $\mathcal{R}^{n \times n}$, the set of real rational transfer functions, and is denoted by P . The transfer function of the controller is denoted by C . The number $\text{wno}(\cdot)$ denotes the winding number of the Nyquist diagram of a scalar transfer function, evaluated on a contour along the imaginary axis and indented to the right around any pure imaginary pole. We will extensively utilize the coprime stable factor representations of P and C , and assume that the plant and all controller transfer functions are always proper. We denote $G(j\omega)^*$ as the complex conjugate transpose of frequency-response function $G(j\omega)$ at each ω , i.e. $G(j\omega)^* = G(-j\omega)^T$.

Definition 1: The unwrapped phase of a scalar transfer function is denoted by unwarg and refers to the phase of the frequency response when it is in the form of a continuous function of the frequency. The unwrapped phase is computed from the phase frequency response by changing absolute jumps greater than π to their 2π complements, and ensures that all appropriate multiples of 2π are included in the phase-frequency response.

Consider the interconnection $[P, C]$ in Fig. 1.

Definition 2: The interconnection $[P, C]$ is “well-posed” if the transfer function matrix mapping $\begin{bmatrix} r \\ w \end{bmatrix}$ to $\begin{bmatrix} y \\ u \end{bmatrix}$ exists. Put another way, $[P, C]$ is well-posed if $(I - CP)^{-1} \in \mathcal{R}$.

Given such well-posedness in Fig. 1 we have

$$\begin{bmatrix} y \\ u \end{bmatrix} = \begin{bmatrix} P \\ I \end{bmatrix} (I - CP)^{-1} \begin{bmatrix} -C & I \end{bmatrix} \begin{bmatrix} r \\ w \end{bmatrix} = H_{[P,C]} \begin{bmatrix} r \\ w \end{bmatrix}.$$

Definition 3: The interconnection $[P, C]$ is said to be “internally stable” if it is well-posed and $H_{[P,C]} \in \mathcal{RH}_\infty$.

We shall define the (2,2) entry of $H_{[P,C]}$ as the *sensitivity matrix*, $S : w \mapsto u$, $S = (I - CP)^{-1}$. Similarly, the (1,1) entry of $H_{[P,C]}$ is defined as the *complementary sensitivity*; i.e. $Q : r \mapsto y$, $Q = -P(I - CP)^{-1}C$ and $Q + S = I$.

Definition 4: The ordered pair $\{N, M\}$, with $M, N \in \mathcal{RH}_\infty$, is a right-coprime factorization (*rcf*) of $P \in \mathcal{R}$ if M is invertible in \mathcal{R} , $P = NM^{-1}$, and N and M are right-coprime over \mathcal{RH}_∞ . Furthermore, the ordered pair $\{N, M\}$ is a normalized *rcf* of P if $\{N, M\}$ is a *rcf* of P and $M^*M + N^*N = I$.

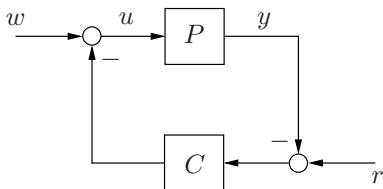


Fig. 1. Standard Feedback Configuration

Definition 5: The ordered pair $\{\tilde{U}, \tilde{V}\}$, with $\tilde{U}, \tilde{V} \in \mathcal{RH}_\infty$, is a left-coprime factorization (*lcf*) of $C \in \mathcal{R}$ if \tilde{V} is invertible in \mathcal{R} , $C = \tilde{V}^{-1}\tilde{U}$, and \tilde{U} and \tilde{V} are left-coprime over \mathcal{RH}_∞ . Furthermore, the ordered pair $\{\tilde{U}, \tilde{V}\}$ is a normalized *lcf* of C if $\{\tilde{U}, \tilde{V}\}$ is a *lcf* and $\tilde{V}\tilde{V}^* + \tilde{U}\tilde{U}^* = I$.

Definition 6:

$$G := \begin{bmatrix} N \\ M \end{bmatrix}, \quad \tilde{K} := [-\tilde{U} \quad \tilde{V}] \quad (1)$$

where G will be referred to as the graph symbol of P , and \tilde{K} will be referred to as the inverse graph symbol of C .

Theorem 7: [12, Proposition 1.9] Let G and \tilde{K} be defined as in (1). Then the following are equivalent:

- i. $[P, C]$ is internally stable;
- ii. $(\tilde{K}G)^{-1} \in \mathcal{RH}_\infty$;
- iii. $\det(\tilde{K}G)(j\omega) \neq 0 \forall \omega$ and $\text{wno} \det(\tilde{K}G) = 0$.

In the sequel we shall refer to standard system performance measures in time (e.g. rise time, overshoot, etc.) and frequency (gain and phase margin etc.) domain defined in [13], [14]. Note that while our methods will apply in the MIMO case, their nice classical control interpretations in the SISO case makes it worthwhile to be highlighted.

III. CONNECTIONS BETWEEN PERFORMANCE MEASURES

We shall establish connections between measures of closed-loop performance to facilitate the development of our proposed performance verification results in the sequel.

A. Performance measures involving $S(s)$ and $Q(s)$

Lemma 8: Let P be scalar in the interconnection in Fig. 1 with loop-gain $G(s) := -P(s)C(s)$. Let PM and GM be the phase-margin and gain-margin of $[P, C]$, and let $M_r^S := \max_\omega |S(j\omega)| = \|S\|_\infty$ and $M_r^Q := \max_\omega |Q(j\omega)| = \|Q\|_\infty$ be the resonant peaks for $S(s)$ and $Q(s)$, respectively. Then:

- $GM \geq \frac{M_r^S}{M_r^S - 1}$;
- $PM \geq 2 \arcsin\left(\frac{1}{2M_r^S}\right) \geq \frac{1}{2M_r^S}$;
- $GM \geq 1 + \frac{1}{M_r^Q}$;
- $PM \geq 2 \arcsin\left(\frac{1}{2M_r^Q}\right) \geq \frac{1}{2M_r^Q}$.

Proof: Let ω_g denote phase-crossover frequency (gain-margin frequency) and ω_p be gain-crossover frequency (phase-margin frequency). Note that $G(j\omega_g) = -1/GM$ since $GM = 1/|G(j\omega_g)|$ and $G(s)$ is real and negative at $j\omega_g$ by definition. Thus $Q(j\omega_g) = -1/(GM - 1)$ and $S(j\omega_g) = 1/(1 - 1/GM)$. Then the related phase-margin results follow.

Further note that

$$|S(j\omega_p)| = 1/|1 + 1/G(j\omega_p)| = 1/|-1 - 1/G(j\omega_p)|$$

and we have

$$|S(j\omega_p)| = |Q(j\omega_p)| = \frac{1}{\sqrt{2(1 - \cos(PM))}} \quad (2)$$

Hence the related phase-margin results follow. ■

Although larger PM and GM leads to a more robust system, one has to observe some trade-offs to ensure a sensible

level of closed-loop performance. For good robustness, it is advised to have $GM > 2$ and $PM > 30^\circ$. The following are direct consequence of the results in Lemma 8:

- $M_r^S = 2$ guarantees $GM \geq 2$ and $PM \geq 29^\circ$;
- $M_r^Q = 2$ guarantees $GM \geq 1.5$ and $PM \geq 29^\circ$;
- For $GM \geq 2$ and $PM \geq 29^\circ$, ensure $M_r^S > 2$.

B. Relationship between GM (or PM) and $\|H_{[P,C]}\|_\infty$

We shall review the established relationships between GM and/or PM with the values of $\|H_{[P,C]}\|_\infty$ discussed in [12].

Definition 9: For a (not necessarily scalar) plant P , the “robust stability margin” $b_{[P,C]}$ is defined by

$$b_{[P,C]} := \begin{cases} \|H_{[P,C]}\|_\infty^{-1}, & \text{if } [P,C] \text{ is stable} \\ 0 & \text{otherwise} \end{cases}$$

Clearly, larger $b_{[P,C]}$ corresponds to the smaller norm, but this norm cannot be smaller than 1 which means that for any P and C , $b_{[P,C]} \in [0, 1]$; see [12].

Remark 10: For a scalar plant, large $b_{[P,C]}$ guarantees small sensitivity at frequencies where $|P(j\omega)|$ is large, and small complementary sensitivity at frequencies where $|P(j\omega)|$ is small. Also, both functions are well behaved around $|P(j\omega)| \approx 1$. The converse is also true.

We also define $\rho(P, C, \omega)$ as a point-wise version of $b_{[P,C]}$.

Definition 11 (P.38 [12]): For $X \in \mathbb{C}^{p \times q}$ and $Z \in \mathbb{C}^{q \times p}$ we define

$$\rho(X, Z, \omega) = 1/\bar{\sigma} \left(\begin{bmatrix} X \\ I \end{bmatrix} (I - ZX)^{-1} \begin{bmatrix} -Z & I \end{bmatrix} \right) (j\omega) \quad (3)$$

Note that if $[P, C]$ is stable,

$$\begin{aligned} \frac{1}{b_{[P,C]}} &= \left\| \begin{bmatrix} P \\ I \end{bmatrix} (I - CP)^{-1} \begin{bmatrix} -C & I \end{bmatrix} \right\|_\infty \\ &= \sup_\omega \left(\left\| \begin{bmatrix} P \\ I \end{bmatrix} (I - CP)^{-1} \begin{bmatrix} -C & I \end{bmatrix} \right\| (j\omega) \right) \\ &= \sup_\omega 1/\rho(P, C, \omega) \end{aligned}$$

and hence

$$b_{[P,C]} = \inf_\omega \rho(P, C, \omega). \quad (4)$$

Since $H_{[P,C]} = G(\tilde{K}G)^{-1}\tilde{K}$, utilizing normalized rcf and lcf descriptions for P and C one obtains

$$\begin{aligned} \rho(P, C, \omega) &= 1/\bar{\sigma}[(G(\tilde{K}G)^{-1}\tilde{K})(j\omega)] \\ &= 1/\bar{\sigma}[(\tilde{K}G)^{-1}(j\omega)] = \underline{\sigma}[(\tilde{K}G)(j\omega)] \end{aligned} \quad (5)$$

Hence, if $[P, C]$ is stable,

$$b_{[P,C]} = 1/\|G(\tilde{K}G)^{-1}\tilde{K}\|_\infty = 1/\|(\tilde{K}G)^{-1}\|_\infty. \quad (6)$$

Theorem 12 ([12]): Suppose P is scalar. If $[P, C] \in \mathcal{RH}_\infty$ then

$$GM_{[P,C]} \geq \frac{(1 + b_{[P,C]})}{(1 - b_{[P,C]})} \text{ and } PM_{[P,C]} \geq 2 \arcsin(b_{[P,C]})$$

Lemma 13 ([15]): Suppose P is scalar. If $[P, C] \in \mathcal{RH}_\infty$, then

$$b_{[P,C]} = \left[(|C| + \frac{1}{|C|})|Q| \right]^{-1}, \quad (7)$$

where $Q = -PC/(1-PC)$ is the complementary sensitivity.

We shall now discuss the problem of interest and pave the way for the introduction of our results.

IV. PROBLEM SET-UP AND PROPOSED ANALYSIS RESULTS

Given a stable closed-loop $[P, C_0]$ consisting of an unknown linear time-invariant (LTI) P and a known LTI C_0 we shall propose tools for verifying the closed-loop performance $[P, C_1]$ before C_1 is switched in.

In order to project the internal stability of $[P, C_1]$ before the insertion of C_1 into the loop, we introduced validation tests in [4], [5], [6] utilizing a limited amount of experimental data obtained from the stable closed-loop interconnection $[P, C_0]$. Our earlier results propose a type of phase test analogous to the Nyquist criterion and utilize the noisy frequency response information of the closed-loop mapping $T : r \mapsto z$ in Fig. 2 to check if C_1 will stabilize the unknown plant P . This was all achieved despite the restrictive assumption that no *a priori* information about the plant was available. This aimed to address the so-called transient instability problem in the context of multiple model adaptive control (MMAC) and iterative identification and control ideas discussed in the introduction. We shall outline the results in [4], [5], [6] (applicable to the MIMO case) for ease of reference.

Theorem 14: Let $[P, C_0]$ be internally stable. Let $C_0 = \tilde{V}_0^{-1}\tilde{U}_0$ and $C_1 = \tilde{V}_1^{-1}\tilde{U}_1$ be left coprime factorizations over \mathcal{RH}_∞ . Consider Fig. 2 and define $T : r \mapsto z$ to be

$$T = \begin{bmatrix} -\tilde{U}_1 & \tilde{V}_1 \end{bmatrix} \begin{bmatrix} P(I - C_0P)^{-1} \\ (I - C_0P)^{-1} \end{bmatrix} \tilde{V}_0^{-1} \quad (8)$$

and let unwarg be the unwrapped phase as in Definition 1. Then the following are equivalent:

- $[P, C_1]$ is internally stable;
- $T^{-1} \in \mathcal{RH}_\infty$;
- $\det T(j\omega) \neq 0 \forall \omega$ AND $\text{wno } \det T = 0$;

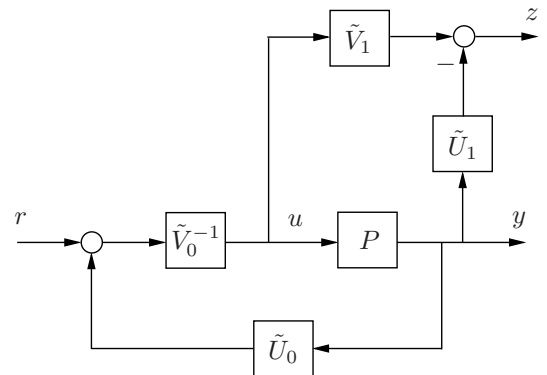


Fig. 2. Experimental setting: $C_0 = \tilde{V}_0^{-1}\tilde{U}_0$, $C_1 = \tilde{V}_1^{-1}\tilde{U}_1$.

d) $\det T(j\omega) \neq 0 \forall \omega$ AND unwarg $\det T(j\infty) = \text{unwarg } \det T(j0)$.

Proof: See [4], [6]. ■

A. Proposed performance analysis results

We shall now build on the stability results in Theorem 14 to gain further insights into the experimental setting of Fig. 2. In particular, we consider the relationship between the closed-loop feedback connection $[P, C_0]$ and the projected interconnection $[P, C_1]$. We work with the same set of assumptions that $[P, C_0]$ is internally stable and let $C_0 = \tilde{V}_0^{-1}\tilde{U}_0$ and $C_1 = \tilde{V}_1^{-1}\tilde{U}_1$ be left coprime factorizations over \mathcal{RH}_∞ and available, but the transfer function of P is unknown.

Note that the mapping $T : r \mapsto z$ in (8) can also be expressed in terms of the graph symbols (see [4], [5], [6] for details) G and \tilde{K}_i given in (1),

$$\begin{aligned} T &= [-\tilde{U}_1 \quad \tilde{V}_1] \begin{bmatrix} P(I - C_0P)^{-1} \\ (I - C_0P)^{-1} \end{bmatrix} \tilde{V}_0^{-1} \\ &= \tilde{K}_1G(\tilde{K}_0G)^{-1}. \end{aligned} \quad (9)$$

From (9), we have $(\tilde{K}_0G)^{-1} = M^{-1}(I - C_0P)^{-1}\tilde{V}_0^{-1}$. Since M is invertible, T can be expressed as

$$\begin{aligned} T &= (\tilde{K}_1G)(\tilde{K}_0G)^{-1} \\ &= [\tilde{V}_1(I - C_1P)M][M^{-1}(I - C_0P)^{-1}\tilde{V}_0^{-1}] \\ &= \tilde{V}_1S_1^{-1}S_0\tilde{V}_0^{-1} \\ &= W_1^{-1}W_0, \end{aligned} \quad (10)$$

where $W_0 = M(\tilde{K}_0G)^{-1}\tilde{V}_0 = (I - C_0P)^{-1}\tilde{V}_0$ is the sensitivity transfer function of the interconnection $[P, C_0]$ in Fig. 2, and $W_1 = M(\tilde{K}_1G)^{-1}\tilde{V}_1 = (I - C_1P)^{-1}\tilde{V}_1$ is the sensitivity transfer function of the interconnection $[P, C_1]$ if C_1 were in the closed-loop.

If $[P, C_i]$ is internally stable, we have $(\tilde{K}_iG)^{-1} \in \mathcal{RH}_\infty$ and the following results hold.

Theorem 15: Suppose the hypothesis of Theorem 14 hold, and consider the setting in Fig. 2. If the conditions (a)–(d) in Theorem 14 are satisfied, then $W_1 = W_0T^{-1} \in \mathcal{RH}_\infty$.

Proof: Since $T = W_1^{-1}W_0$, one can express

$$T^{-1} := W_0^{-1}W_1. \quad (11)$$

Since $[P, C_0] \in \mathcal{RH}_\infty$, we have $(\tilde{K}_0G)^{-1} \in \mathcal{RH}_\infty$. Also, we have $M \in \mathcal{RH}_\infty$. Hence $W_0 = M(\tilde{K}_0G)^{-1} \in \mathcal{RH}_\infty$. Now pre- and post-multiplying (11) by S_0 , one obtains $W_0T^{-1} := W_1$. We shall show that $W_1 \in \mathcal{RH}_\infty$. From the condition (b), $T^{-1} \in \mathcal{RH}_\infty$. Since $W_0 \in \mathcal{RH}_\infty$, we have $W_1 = W_0T^{-1} \in \mathcal{RH}_\infty$. ■

The aforementioned results in Theorems 15 can be utilized to verify the performance of W_1 given the performance aspects of W_0 and T^{-1} are available. In the following section, these results will be expanded for our proposed performance verification test to project some performance aspects with C_1 prior to its actual insertion into the closed-loop, given that the transfer function of P is unknown.

B. Proposed performance analysis: bounds on $\|H_{[P,C]}\|_\infty$

The following results utilize the norms of $[P, C_0]$ and $[P, C_1]$ as performance indices.

Theorem 16: Let $[P, C_0] \in \mathcal{RH}_\infty$ and $C_0 = \tilde{V}_0^{-1}\tilde{U}_0$ and $C_1 = \tilde{V}_1^{-1}\tilde{U}_1$ be left coprime factorizations over \mathcal{RH}_∞ . Consider the configuration in Fig. 2 and define the mapping $T : r \mapsto z$ to be as in (8). Let $b_{[P,C_0]}$ and $b_{[P,C_1]}$ be indices for $[P, C_0]$ and $[P, C_1]$ as in Definition 9. If $[P, C_1]$ is internally stable, we have

$$b_{[P,C_0]}\|T^{-1}\|_\infty^{-1} \leq b_{[P,C_1]} \leq b_{[P,C_0]}\|T\|_\infty. \quad (12)$$

Proof: From (9), we have $T = \tilde{K}_1G(\tilde{K}_0G)^{-1}$. If $[P, C_1]$ is internally stable, $(\tilde{K}_1G)^{-1}$ exists, and $(\tilde{K}_1G)^{-1}T = (\tilde{K}_0G)^{-1}$. Hence,

$$\begin{aligned} \|(\tilde{K}_1G)^{-1}T\|_\infty &= \|(\tilde{K}_0G)^{-1}\|_\infty \\ \Rightarrow \|(\tilde{K}_1G)^{-1}\|_\infty\|T\|_\infty &\geq \|(\tilde{K}_0G)^{-1}\|_\infty \\ \Rightarrow b_{[P,C_1]}^{-1}\|T\|_\infty &\geq b_{[P,C_0]}^{-1} \end{aligned}$$

Thus, $b_{[P,C_1]} \leq b_{[P,C_0]}\|T\|_\infty$ holds.

If $[P, C_1]$ is internally stable, T^{-1} exists (via Theorem 14), and $(\tilde{K}_1G)^{-1} = (\tilde{K}_0G)^{-1}T^{-1}$. As a result,

$$\begin{aligned} \|(\tilde{K}_1G)^{-1}\|_\infty &\leq \|(\tilde{K}_0G)^{-1}\|_\infty\|T^{-1}\|_\infty \\ \Rightarrow b_{[P,C_1]}^{-1} &\leq b_{[P,C_0]}^{-1}\|T^{-1}\|_\infty \end{aligned}$$

Thus, the inequality $b_{[P,C_1]} \geq b_{[P,C_0]}\|T^{-1}\|_\infty^{-1}$ holds. ■

Remark 17: The results in Theorem 16 is a flag indicating that the sensitivity of closed-loop $[P, C_1]$ might be very bad if $\|T\|$ can get very small, but will not be very bad in the contrary case.

The pointwise version of Theorem 16 is given below.

Theorem 18: Suppose the hypothesis of Theorem 16 holds and consider the configuration in Fig. 2. Define the mapping $T : r \mapsto z$ as in (8). The following holds $\forall \omega$,

$$\begin{aligned} \frac{1}{\bar{\sigma}[T^{-1}(j\omega)]}\rho(P, C_0, \omega) &\leq \rho(P, C_1, \omega) \\ &\leq \bar{\sigma}[T(j\omega)]\rho(P, C_0, \omega). \end{aligned} \quad (13)$$

Proof: From (9), we have

$$(T\tilde{K}_0G)(j\omega) = (\tilde{K}_1G)(j\omega). \quad (14)$$

and

$$\begin{aligned} \underline{\sigma}[(T\tilde{K}_0G)(j\omega)] &= \underline{\sigma}[(\tilde{K}_1G)(j\omega)] \\ \Rightarrow \underline{\sigma}[T(j\omega)]\underline{\sigma}[(\tilde{K}_0G)(j\omega)] &\leq \underline{\sigma}[(\tilde{K}_1G)(j\omega)] \end{aligned}$$

Since $\underline{\sigma}[(\tilde{K}_iG)(j\omega)] = \rho(P, C_i)$ as shown in (5) and $\underline{\sigma}[T(j\omega)] = 1/\bar{\sigma}[T^{-1}(j\omega)]$, the inequality $\frac{1}{\bar{\sigma}[T^{-1}(j\omega)]}\rho(P, C_0, \omega) \leq \rho(P, C_1, \omega)$ holds.

Similarly,

$$(T^{-1}\tilde{K}_1G)(j\omega) = (\tilde{K}_0G)(j\omega). \quad (15)$$

and

$$\begin{aligned} \underline{\sigma}[(T^{-1}\tilde{K}_1G)(j\omega)] &= \underline{\sigma}[(\tilde{K}_0G)(j\omega)] \\ \Rightarrow \underline{\sigma}[T^{-1}(j\omega)]\underline{\sigma}[(\tilde{K}_1G)(j\omega)] &\leq \underline{\sigma}[(\tilde{K}_0G)(j\omega)] \end{aligned}$$

Thus, the inequality $\rho(P, C_1, \omega) \leq \bar{\sigma}[T(j\omega)]\rho(P, C_0, \omega)$ holds. ■

Note that if the system is restricted to be Single-Input Single-Output (SISO), the inequality in the above Theorem becomes an equality.

Theorem 19: Suppose P is scalar in Fig. 2 and the hypothesis of Theorem 16 holds. Define $T : r \mapsto z$ (8). For SISO systems, we have

$$|T(j\omega)|\rho(P, C_0, \omega) = \rho(P, C_1, \omega) \quad \forall \omega. \quad (16)$$

Proof: From (9), we have

$$(T\tilde{K}_0G)(j\omega) = (\tilde{K}_1G)(j\omega) \quad \forall \omega. \quad (17)$$

This implies that

$$\underline{\sigma}[(T\tilde{K}_0G)(j\omega)] = \underline{\sigma}[(\tilde{K}_1G)(j\omega)] \quad \forall \omega. \quad (18)$$

Since $T(j\omega)$ is a scalar for SISO systems (ie. $|T(j\omega)|$ can be factored out) and using (5) (ie. $\rho(P, C_i, \omega) = \underline{\sigma}[\tilde{K}_iG(j\omega)]$), we get

$$|T(j\omega)|\rho(P, C_0) = \rho(P, C_1). \quad (19)$$

■
Corollary 20: Suppose P is scalar in Fig. 2 and the hypothesis of Theorem 16 hold. If $[P, C_1]$ is internally stable, we have

- $GM_{[P, C_1]} \geq \frac{1+b_{[P, C_0]}\|T^{-1}\|_{\infty}^{-1}}{1-b_{[P, C_0]}\|T\|_{\infty}}$;
- $PM_{[P, C_1]} \geq 2 \arcsin(b_{[P, C_0]}\|T^{-1}\|_{\infty}^{-1})$.

Proof: The results follow straight from Theorem 12 and Theorem 16. ■

V. PERFORMANCE VERIFICATION OF $[P, C_1]$

Let us recall that we aim to verify the closed-loop performance of $[P, C_1]$ in advance of the insertion of C_1 into the loop knowing that $[P, C_0]$ is internally stable, P is unknown and C_0 and C_1 are available. We also have novel tools at our disposal for projecting internal stability of $[P, C_1]$.

We shall develop experimental tests which utilise the closed-loop data from the stable interconnection $[P, C_0]$ and information about C_0 and C_1 to enable measuring some performance aspects of $[P, C_1]$. We assume that the signals r , u and z are accessible for measurement, and let u_{ss} and z_{ss} denote the steady-state of $u(t)$ and $z(t)$, respectively. Note that for a stable system $y = Gu$ sinusoidal steady-state response can be expressed as $y_{ss}(t) = |G(j\omega)| \cos(\omega t + \angle G(j\omega))$. The response to a sinusoidal input is asymptotically sinusoidal, with the same frequency as the input, and with magnitude $|G(j\omega)|$ determining the amplification factor, i.e. $\text{RMS}(y_{ss})/\text{RMS}(u)$, and phase $\angle G(j\omega)$ indicating the phase shift between u and y_{ss} .

In our framework, $[P, C_1]$ is internally stable,

$$W_1(j\omega) = W_0(j\omega)T^{-1}(j\omega), \quad \forall \omega$$

via Theorem 15. At each frequency, this relationship facilitates the computation of $|W_1(j\omega)|$ and $\angle W_1(j\omega)$ using the aforementioned standard mechanism for obtaining the magnitude and phase of $W_0(j\omega)$ and $T(j\omega)$.

Note that verifying the performance of $[P, C_1]$ does not require the full frequency response of W_1 , but some frequency-domain characteristics as discussed in Section IV. The following procedures can be utilized to project the phase margin (PM) and gain margin (GM) of $[P, C_1]$, and then infer further performance aspects via the connections discussed in Section III.

Algorithm 21 (Projecting Phase Margin with C_1):

Suppose the hypothesis of Theorem 14 hold, and consider the setting in Fig. 2.

- Step 1: Ensure $[P, C_1]$ is internally stable via data-based tests proposed in [4], [5], [6];
- Step 2: Set frequency $\omega = 0$.
- Step 3: Insert a sinusoidal signal of frequency ω at reference input r while other input $w = 0$;
- Step 4: Compute u_{ss} and z_{ss} using the method discussed in the preceding paragraphs, and obtain $|W_1(j\omega)|$ at each frequency ω ;
- Step 5: If $|W_1(j\omega)| = 1$, set $\omega_p = \omega$ and go to Step 6; otherwise increase ω by ω_{Δ} (the step size of the frequency grid) and go to Step 3.
- Step 6: Measure $\angle W_1$ at ω_p by computing the phase difference between u and z ;
- Step 7: Phase Margin of $[P, C_1]$ is $(180^\circ - \angle W_1)$.

Algorithm 22 (Projecting Gain Margin with C_1):

Suppose the hypothesis of Theorem 14 hold, and consider the setting in Fig. 2.

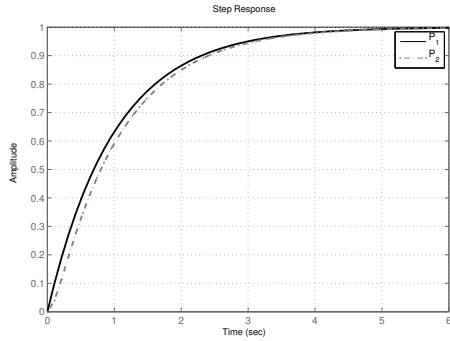
- Step 1: Ensure $[P, C_1]$ is internally stable via data-based tests proposed in [4], [5], [6];
- Step 2: Set frequency $\omega = 0$.
- Step 3: Insert a sinusoidal signal of frequency ω at reference input r while other input $w = 0$;
- Step 4: Compute phase shift between u and z at steady state using the method discussed in the preceding paragraphs, and obtain $\angle W_1(j\omega)$ at each frequency ω ;
- Step 5: If $\angle W_1(j\omega) = -180^\circ$, set $\omega_g = \omega$ and go to Step 6; otherwise increase ω by ω_{Δ} (the step size of the frequency grid) and go to Step 3.
- Step 6: Measure $|W_1|$ at ω_g ;
- Step 7: Gain Margin of $[P, C_1]$ is $-20 \log_{10} |W_1|$.

The above procedures for projecting the Phase and Gain Margins of $[P, C_1]$ require calculations over a limited frequency ranges, i.e. $\omega \in [0, \omega_p]$ and $\omega \in [0, \omega_g]$.

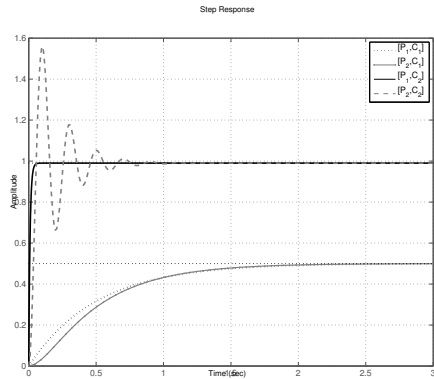
Similar procedures could be developed for determining the Bandwidth, M_r and other frequency-domain characteristics of $[P, C_1]$ exploring the properties of W_1 . One can also utilise the indirect measurement results in Lemma 16 and Corollary 20 to determine lower bounds on PM and GM of $[P, C_1]$.

VI. ILLUSTRATIVE EXAMPLE

Let us consider the example discussed in the introduction again. Let a second order plant $P_1(s) = 1/(s+1)(.1s+1)$ be approximated by $P_2(s) = 1/(s+1)$. Let $C_1 = -1$ and $C_2 = -100$ be candidate controllers which both would give good performance for the model P_2 . This is illustrated in Fig. 3.



(a) Plant and Model responses in Open Loop



(b) Plant and Model responses in Closed Loop

Fig. 3. Comparison of step responses

For illustration purposes and due to space limitation, let us consider a simple scenario. Consider Fig. 2 and assume $C_0 = 0$ and construct $T : r \mapsto z$ with the controller C_1 as a potential replacement. We shall denote this mapping as T_1 . Similarly, let us denote T_2 the mapping resulting from C_2 . The Nyquist diagrams of T_1 and T_2 are shown in Fig. 4.

Note that the study of T in Fig. 4 with both the proposed controllers and the plant P_1 shows that $|T|$ gets very close to zero with C_2 , illustrating that performance may be severely degraded.

VII. CONCLUSIONS

We have proposed performance validation tests for linear time-invariant systems which aim to project aspects of closed-loop performance with the introduction of a new controller C_1 via utilizing a limited amount of experimental data obtained from the stable closed-loop interconnection $[P, C_0]$. Our earlier results in [4], [5], [6] verify that C_1 will be stabilizing (in place of C_0) if the Nyquist plot of $T : r \mapsto z$ in Fig. 2 does not encircle the origin.

Our proposed results in this manuscript project performance aspects of the closed-loop with C_1 in advance of its insertion into the closed-loop and raise the red flag if, for example, at frequencies T has small magnitude. Also, bounds on potential damage have been developed.

We have also extended our LTI stability results to the nonlinear case in [7], [8], [9] and developed analysis results.

Using the kernel representations and the small gain theorem, we further achieved an additional data-based test to guarantee internal stability of $[P, C_1]$ where the nonlinear C_1 has a special structure.

REFERENCES

- [1] A. S. Morse, "Supervisory control of families of linear set-point controller part i. exact matching," *IEEE Transactions on Automatic Control*, vol. 41, no. 10, pp. 1413–1431, 1996.
- [2] K. S. Narendra and J. Balakrishnan, "Adaptive control using multiple models," *IEEE Transactions on Automatic Control*, vol. 42, pp. 171–187, 1997.
- [3] B. D. Anderson and A. Dehghani, "Challenges of adaptive control-past, permanent and future," *Annual Reviews in Control*, vol. 32, no. 2, pp. 123 – 135, 2008.
- [4] A. Dehghani, B. D. O. Anderson, A. Lanzon, and A. Lecchini-Visintini, "Verifying stabilizing controllers via closed-loop noisy data: MIMO case," in *Proceedings of the 46th IEEE Conference on Decision and Control*, New Orleans, LA, USA, December 2007.
- [5] A. Dehghani, B. D. O. Anderson, and R. A. Kennedy, "Practical novel tests for ensuring safe adaptive control," in *Proceedings of the 47th IEEE Conference on Decision and Control*, Cancun, Mexico, Dec. 2008, pp. 708–713.
- [6] A. Dehghani, A. Lecchini, A. Lanzon, and B. D. O. Anderson, "Validating controllers for internal stability utilizing closed-loop data," *IEEE Transactions on Automatic Control*, vol. 54, no. 11, November 2009.
- [7] S. H. Cha, A. Dehghani, and B. D. O. Anderson, "Safe nonlinear controller design with biomedical engineering applications," in *Proceedings of the 7th Asian Control Conference*, 2009.
- [8] —, "Verifying nonlinear controllers for stability utilizing closed-loop noisy data," in *Proceedings of the 48th IEEE Conference on Decision and Control*, 2009, submitted.
- [9] —, "Nonlinear analysis for verifying closed-loop stability before inserting a new controller," in *Proceedings of the 10th European Control Conference*, 2009.
- [10] K. Zhou and J. C. Doyle, *Essentials of robust control*. Prentice-Hall, 1997.
- [11] N. Linard, B. D. O. Anderson, and F. De Bruyne, "Identification of a nonlinear plant under nonlinear feedback using left coprime fractional based representation," *Automatica*, vol. 35, no. 4, pp. 655–668, 1999.
- [12] G. Vinnicombe, *Uncertainty and feedback: \mathcal{H}_∞ loop-shaping and the v -gap metric*. Imperial College Press, 2000.
- [13] G. C. Goodwin, S. F. Graebe, and M. E. Salgado, *Control System Design*. Prentice-Hall, 2001.
- [14] G. F. Franklin, J. D. Powell, and A. Emami-Naeini, *Feedback Control of Dynamic Systems*, 5th ed. Prentice-Hall, 2006.
- [15] A. Dehghani, A. Lanzon, and B. D. O. Anderson, "An \mathcal{H}_∞ algorithm for the windsurfer approach to adaptive robust control," *International Journal of Adaptive Control and Signal Processing*, vol. 18, no. 8, pp. 607–628, Oct. 2004.

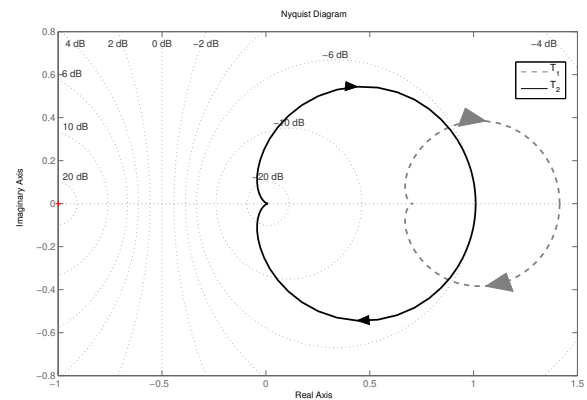


Fig. 4. Nyquist diagrams of T_1 and T_2